Civil Engineering Infrastructures Journal 2022, 55(2): 309-331
DOI: 10.22059/CEIJ.2021.325512.1760

RESEARCH PAPER

Structural Control of Building with ATMD through AN-IT2FLC under Seismic Excitation

Golnargesi, S.[1*], Shariatmadar, H.[2] and Golnargesi, B.[3]

[1] Assistant Professor, Faculty of Civil Engineering and Environment, Khavaran Institute of Higher Education, Mashhad, Iran.
[2] Professor, Faculty of Civil Engineering, Ferdowsi University, Mashhad, Iran.
[3] Ph.D. Candidate, Islamic Azad University, Mashhad Branch, Mashhad, Iran.

© University of Tehran 2022

Received: 13 Jun. 2021; Revised: 15 Sep. 2021; Accepted: 26 Sep. 2021

ABSTRACT: This paper focuses on the design of Adaptive-Neural Interval Type-2 Fuzzy Logic Controller (AN-IT2FLC) in an active tuned mass damper to reduce the response of building under seismic excitation. One of the main shortcomings of Interval Type-2 Fuzzy Logic Controller (IT2FLC) is its need to adjust in any earthquake. This is whilst the AN-IT2FLC can solve this problem using the training process. In this research, four inputs are used for designing and training of AN-IT2FLC as controlled displacement and velocity of roof level with IT2FLC, acceleration of the implemented earthquakes and the control force of IT2FLC. AN-IT2FLC training performed based on the eight earthquake records of El Centro, Hachinohe, Kobe, Northridge, Loma Prieta, Tabas, Morgan Hill and Erizkan with various seismic characteristics. In order to investigate the effectiveness of the proposed controller, an 11-story building with ATMD on its top floor analyzed under another four ground accelerations of Chi-Chi, Kern-county, Coalinga and Coyote-lake records. The results revealed that ATMD with AN-IT2FLC is able to achieve more response reduction with higher speed and accuracy rather than that of the IT2FLC.

Keywords: AN-IT2FLC, ATMD, Earthquake Excitation, Structural Control.

1. Introduction

It is inevitable that natural disasters such as earthquakes cause damage to the structures unpredictably. The earthquake excitations must be damped in some way to minimize possible damages to the building. The use of structural control systems can help the structural designers to achieve this aim. So far, various types of structural control systems and devices have been proposed, which are divided into four general categories according to the type of operation as passive, active, semi-active, and hybrid. Due to their simple application and high reliability, passive control methods are widely used. One of the most effective devices of passive control is the Tuned Mass Damper (TMD), which attracted many researchers' attention (Farshidianfar and Soheili, 2013; Meshkat Razavi and Shariatmadar, 2015; Ying Zhou et al., 2019; Ying Zhou et al., 2020; Love and Haskett, 2019; Anajafi and Medina, 2017; Miguel et al., 2016; Lievens et al., 2016; Zuo et al., 2021; Jin et al., 2020; Huang et al., 2020;

* Corresponding author E-mail: golnargesi.siamak@gmail.com

Boccamazzo et al., 2020).

Extensive efforts have been done to increase the capacity of TMD, including setup of an active control force between the building and the TMD. This new control system is called "Active Tuned Mass Damper" (ATMD). By surveying the structural control concepts, it can be found that the ATMD which is used in this study is a hybrid control device.

The role of the hybrid control system is to reduce building vibration under seismic loadings with uncertain characteristics such as strong winds and highly damaging earthquake excitations and consequently to increase comfort of occupants of the building.

A hybrid control system may use active control to supplement and improve the performance of a passive control system and because double control devices are operating in it (e.g. in an ATMD) it can alleviate some of the restrictions and limitations that exist when each system is acting alone. In the other hands, a hybrid control device is typically defined as one that utilizes a combination of passive and active systems where in the passive control may be added to an active control scheme to decrease its energy requirements. For example, the mass damper and actuator are the passive and active devices in an ATMD, respectively.

It should be noted in passing that one of the essential differences between an active and a hybrid control scheme, in many cases, is the amount of external energy used to implement control force which is much less in the hybrid control system. In this regard, a side benefit of hybrid control device is that, in the case of a power failure, the passive component of the control still offers some degree of protection, unlike an active control system. Thus, higher levels of performance may be achievable and the overall reliability and efficiency of the controlled structure is increased.

After reviewing the superiority of hybrid control system over its active and passive, its advantages are compared with semi-active ones, in the following:

- Semi-active devices composed of materials with variable characteristic (such as viscosity) which may change its properties during operation and makes them to be unreliable.
- Practical design of a semi-active system using conventional technologies is under the constraints of weight, size and cost.
- Design of semi-active devices involves many mechanical and electrical components that puts limit on the tuning range of the resonance frequency of the device.

Because of the mentioned comparative disadvantages of semi-active systems, the use of hybrid control devices such as ATMD is recommended for the optimal control objectives.

Finally, in comparison with other control systems, a number of advantages associated with hybrid control systems can be cited as:

- Enhanced effectiveness in response control;
- Relative insensitivity to site conditions and ground excitations;
- Applicability to multi-hazard mitigation situations;
- Control objective selectivity.

For example, in the latter, while the main objective is to increase structural safety during severe earthquakes, human comfort should also be emphasized over other aspects of structural motion during noncritical times (Soong and Reinhorn, 1993; Housner et al., 1997; Spencer and Nagarajaiah, 2003; Bathaei et al., 2017; Wang et al., 2021; Ying Zhou et al., 2020).

This is why several theoretical and laboratory studies have been done to find the optimal actuator force to reduce the response of the buildings. For the first time, Kobori et al. (1991) used an ATMD to reduce the response of a real 10-story building under external forces of earthquake and wind. Theoretical studies have been carried out on the active mass damper in two general fields of mathematical research and artificial intelligence. Among the mathematical studies, the Linear Quadratic Regulator (LQR) optimize control (Chang and Soong, 1980), the pole assignment and the Bang-Bang (Collins and Basu, 2006) control strategies can be mentioned. Also, numerous studies are conducted in the field of fuzzy systems, neural networks and adaptive-neural fuzzy systems, some of which are referred as below:

Guclu and Yazici (2008) compared fuzzy and Proportional-Derivative (PD) controllers in a 15-story building. Optimization of fuzzy membership functions in an ATMD controller accomplished by Pourzeinali et al. (2007), through using genetic algorithm to optimize fuzzy controller parameters. The results revealed that the fuzzy optimized controller has a much better behavior compared to the LQR controller. In order to reach synthetic artificial accelerograms with response spectrum similar to the target spectrum, combination of neural networks and wavelets used by Bargi et al. (2012). Golnargesi et al. (2014), modeled the interval type 2 FLC in an active tuned mass damper for seismic control of buildings. One of the weak points of the conventional fuzzy systems (FLS) is the lack of consideration of the uncertainty in fuzzy rules. Type 2 fuzzy systems are capable of considering this kind of uncertainty. Their research deduced that the interval type 2 FLC is more effective than the FLC in mitigating the response of the building. Naderpour et al. (2016) used a suitable neural network to estimate the dispersion of far-field earthquake disturbances. The results showed that the trained neural network has an acceptable accuracy compared with the finite element models. Golnargesi et al. (2018) investigated the seismic control of buildings with ATMD using interval type2 FLC, including soil-structure interaction. They analyzed the structural response in two conditions, with and without considering the Soil-Structure Interaction (SSI) effects. Their research results demonstrated that considering soil type effects has a significant impression on structural responses. Chen et al. (2019) used EB algorithm to optimize the controlling system. They showed that the proposed method is more useful for closed loop control systems. Bakhshinezhad and Mohebbi (2019) developed the fragility curves of buildings with SATMD by considering uncertainties of different parameters. The results included that STMD improves the performance of seismic fragility of nonlinear buildings.

Considering the studies carried out in this field, it can be concluded that there has not been undertaken any similar research on the use of interval type 2 fuzzy systems and neural networks simultaneously to control the structural responses and it is the innovation of this research which will be expressed in the following.

The aim of the present study is to design a new active control system to reduce the seismic response of buildings, called the Adaptive-Neural Interval Type 2 Fuzzy Logic System (AN-IT2FLS). For this purpose, an ATMD with AN-IT2FLC is installed on the top floor of an 11-story shear building and the proposed control system is trained using eight various earthquakes. Therefore, to investigate the efficiency of the proposed control algorithm, the building is analyzed under two far-field earthquakes (Kern-county and Chi-Chi) and two near-field earthquakes (Coalinga and Coyote-lake), where structural responses are obtained in different control cases. The results indicate the high ability, accuracy and speed of processing of AN-IT2FLC in mitigating building response compared to IT2FLC with optimum general parameters in different types of earthquake records.

2. Modeling and Numerical Example

An n-story shear building, along with an ATMD on its roof level, can be considered as a (n+1) degrees of freedom building (Figure 1).

The equation of motion of the above system under seismic excitations is as Eq.

(1), in which M, K and C: are the matrices of mass, stiffness and damping of the building, U: is the horizontal displacement vector of stories toward the ground, E: is the effect vector, a_g: is the ground acceleration, E_f: is the position vector of the control force and F: is the control force.

$$M.\ddot{U}(t) + C.\dot{U}(t) + K.U(t) = -M.E.a_g + E_f.F \tag{1}$$

$$U(t) = \{u_1(t), u_2(t), \dots, u_n(t), u_d(t)\} \tag{2}$$

$$M = diag[m_1, m_2, \dots, m_n, m_d] \tag{3}$$

$$K = \begin{bmatrix} K_1+K_2 & -K_2 & 0 & \cdots & 0 \\ -K_2 & K_2+K_3 & & & \vdots \\ \vdots & 0 & \cdots & -K_n & 0 \\ & \vdots & -K_n & K_n+K_d & -K_d \\ 0 & \cdots & 0 & -K_d & K_d \end{bmatrix} \tag{4}$$

$$C = \begin{bmatrix} C_1+C_2 & -C_2 & 0 & \cdots & 0 \\ -C_2 & C_2+C_3 & & & \vdots \\ \vdots & 0 & \cdots & -C_n & 0 \\ & \vdots & -C_n & C_n+C_d & -C_d \\ 0 & \cdots & 0 & -C_d & C_d \end{bmatrix} \tag{5}$$

$$E = \{1, 1, \dots, 1\}^T_{((n+1)\times 1)} \tag{6}$$

$$Ef = \begin{bmatrix} [0]_{(n-1)\times 1} \\ -1 \\ 1 \end{bmatrix} \tag{7}$$

where in the K and C matrices, K_d: is the mass damper stiffness and C_d: is the damping coefficient of the mass damper. Eq. (1) can be written in the form of the space state as follows:

$$\dot{X} = A.X + B_f.F + B_g.a_g \tag{8}$$

where X: is a vector of (n+1) order, and is defined with A, B_f, B_g in the following equations:

$$X = \begin{Bmatrix} \{u\}_{(n+1)\times 1} \\ \{\{\dot{u}\}_{(n+1)\times 1}\} \end{Bmatrix} \tag{9}$$

$$A = \begin{bmatrix} [0]_{(n+1)\times(n+1)} & [I]_{(n+1)\times(n+1)} \\ [-M^{-1}.K]_{(n+1)\times(n+1)} & [-M^{-1}.C]_{(n+1)\times(n+1)} \end{bmatrix} \tag{10}$$

$$Bf = \begin{Bmatrix} \{0\}_{(n+1)\times 1} \\ \{-M^{-1}.E_f\}_{(n+1)\times 1} \end{Bmatrix} \tag{11}$$

$$Bg = \begin{Bmatrix} \{0\}_{(n+1)\times 1} \\ \{-E\}_{(n+1)\times 1} \end{Bmatrix} \tag{12}$$

The used building in this paper is an 11-story shear building (Figure 2) located in Rasht city of Iran with an ATMD on the last floor (Pourzeinali et al., 2007). The structural characteristics of the building (stiffness and mass of stories) are listed in Table 1.

The structural damping matrix is calculated according to the Rayleigh's method. Considering the damping ratio of the building as the 5% of critical damping value for the first and second modes, calculation of damping matrix can be done as follows (Pourzeinali et al., 2007):

$$C = X_1.[M] + X_2.[K] \tag{13}$$

$$X_1 = \xi\left(\frac{2\omega_1.\omega_2}{\omega_1+\omega_2}\right) \quad , \quad X_2 = \xi\left(\frac{2}{\omega_1+\omega_2}\right) \tag{14}$$

where, ω_1 and ω_2: are the first two natural frequencies of the uncontrolled structure and calculated as 6.5727 and 19.355 (rad/s), respectively.

3. Adaptive-Neural Interval Type-2 Fuzzy Logic Systems (AN-IT2FLS)

Jang (1993) presented the adaptive neural fuzzy inference system (ANFIS). This system is a simple learning technique uses fuzzy algorithms to convert inputs given to a desired output through the processing of information. ANFIS is a combination of both fuzzy and neural networks and integrates both into a single method simultaneously. In this method, the parameters of the fuzzy inference system are adjusted using neural networks.

Since different rules cannot share the same output function, and the number of membership functions must be equal to the number of rules, it is possible to use the architecture of a neuro-fuzzy system from two IF-THEN fuzzy rules, based on a first-order model (Eqs. (15) and (16)).

$$Rule_{(1)}: IF\ x\ is\ A_1\ AND\ y\ is\ B_1 ، THEN\ \ f_1 = p_1 x + q_1 y + r_1 \tag{15}$$

$$Rule_{(2)}: IF\ x\ is\ A_2\ AND\ y\ is\ B_2 ، THEN\ \ f_2 = p_2 x + q_2 y + r_2 \tag{16}$$

where X and Y: are system input, A_i and B_i: are fuzzy sets, f_i: is fuzzy outputs obtained from fuzzy rule, p_i, q_i and r_i: are design parameters during the training process. The architecture of ANFIS for implementing these two rules is clear in Figure 3.

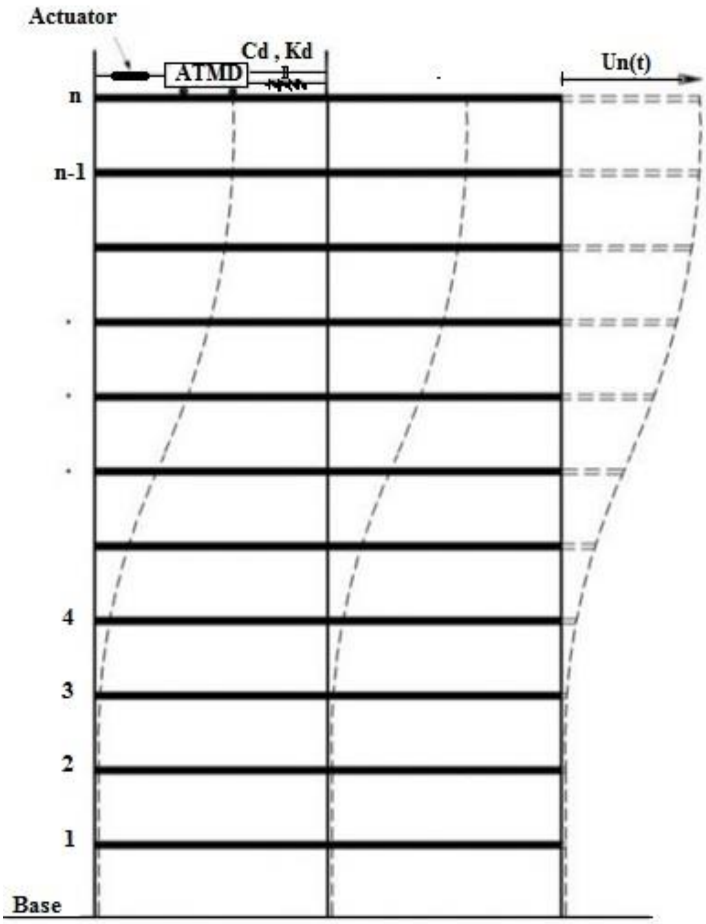

Fig. 1. n-story shear building with ATMD on the top floor

Table 1. Mass and stiffness of building stories

Floor	Stiffness (N/m)	Mass (kg)
1	4.68e8	21537
2	4.76e8	201750
3	4.68e8	201750
4	4.5e8	200930
5	4.5e8	200930
6	4.5e8	200930
7	4.5e8	203180
8	4.37e8	202910
9	4.37e8	202910
10	4.37e8	176100
11	3.12e8	66230

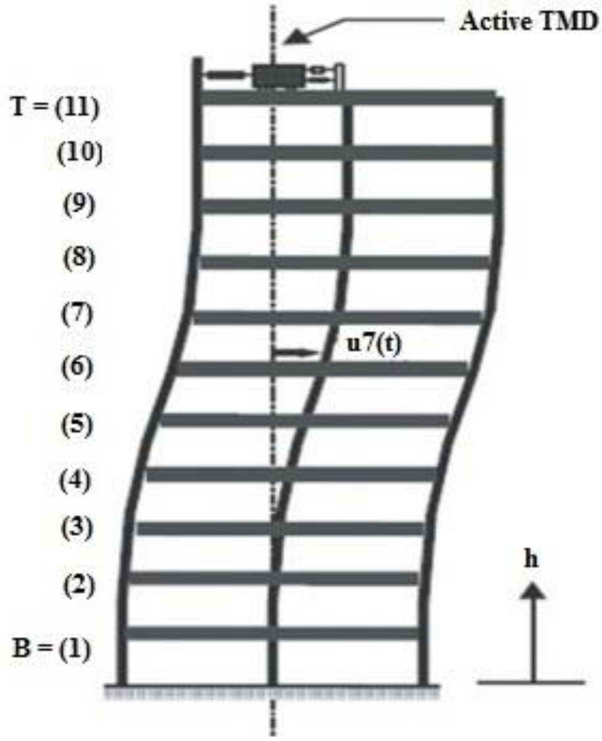

Fig. 2. The 11-story building with ATMD

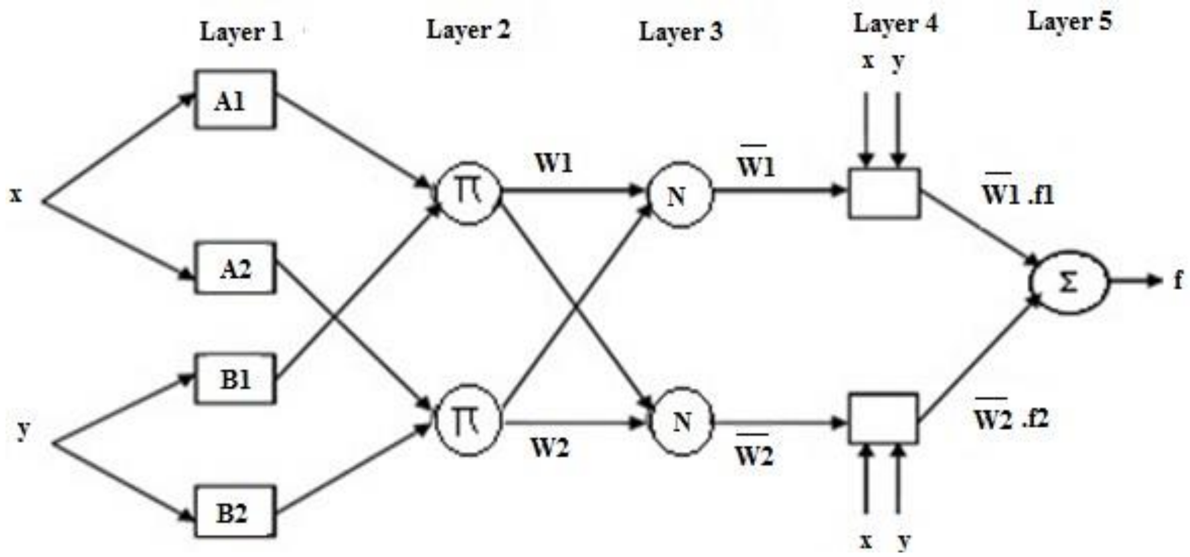

Fig. 3. ANFIS Architecture

According to Figure 3, the circle sign represents a fixed node and the square sign indicates the consistent node. Also from the Figure 2, it can be seen that ANFIS architecture has 5 layers. In Layer 1, all are compatible nodes. The outputs of the Layer 1 are the degrees of membership of the fuzzy inputs, which can be seen in Eqs. (17) and (18):

$$O_{1,i} = \mu_{Ai}(x) \text{ ، } i = 1،2 \quad (17)$$

$$O_{1,i} = \mu_{Bi-2}(y) \text{ ، } i = 3،4 \quad (18)$$

In this layer, X and Y: are its node inputs, and A_i and B_i: are defined as parameters associated with the μ_{Ai} *(x)* and $\mu_{(Bi-2)}$ *(y)* functions. In Layer 2, nodes are considered to be constant. This layer contains fuzzy operators that are represented by the π parameter and act as a simple coefficient. The output of this layer is represented by Eq. (19):

$$O_{2,i} = w_i = \mu_{Ai}(x) * \mu_{Bi}(y) \text{ ، } i = 1، 2 \quad (19)$$

in Layer 3, the fixed nodes are shown with the parameter *N* and play a normalize role rather than the previous layer. The output of this layer can be expressed as Eq. (20):

$$O_{3,i} = \bar{w}_i = \frac{w_i}{w_1 + w_2} , i = 1,2 \quad (20)$$

Regarding the Eq. (21), the fourth layer, composed of product of normalized weight of each fuzzy rule and the output of the last part of that rule.

$$O_{4,i} = \bar{w}_i f_i = \bar{w}_i (p_i x + q_i y + r_i) , i = 1,2 \quad (21)$$

in such a way that $\bar{w}_i$: is the output of the third layer, and p_i, q_i and r_i: are defined as the corresponding parameters.

In the fifth layer, there is only one fixed node with the sign Σ, which represents the total input signals. The total output of the ANFIS is seen in Eq. (22).

$$O_{5,i} = \sum_i \bar{w} f_i = \frac{\sum_i w_i f_i}{\sum_i w_i} \quad (22)$$

Now, if the Interval Type-2 Fuzzy Inference System (IT2FIS) used in ANFIS introduced in this section, Adaptive-Neural Interval Type-2 Fuzzy Inference System (AN-IT2FIS) will be obtained, which will be followed by its design and how it will be modelled.

4. AN-IT2FLC Training and Design

In this paper, the training Process of AN-IT2FLC, is done by gradient descent algorithm. The main advantages of this learning algorithm are the fast and well fitness of training data and simplicity of iterative formula for the computation.

In the following, for the learning of fuzzy rules and membership functions of AN-IT2FLC the mentioned algorithm is expressed (Ichihashi, 1991; Kosko, 1992; Yager and Filev, 1994). For a given fuzzy system model with a number of input variables ($x_1, x_2, ..., x_n$) and one output variable (y), the fuzzy rule base is defined as follows (Ichihashi, 1991; Kosko, 1992):

Rule i: If x_1 *is* A_{1i} *and* x_2 *is* A_{2i} *... and* x_n*, is* A_{ni}*, Then y is* y_i $(i = 1, 2, ..., m)$ (23)

where A_{ji} (j=1, 2, …, n and i=1, 2, …, m): is a membership function for the input variable x_j which is expressed in Eq. (27), y_i is a real number on the output universe *Y*, and *m*: is the number of the fuzzy rules.

$$Aji(x_j) = exp(-(x_j - a_{ji})^2 / b_{ji}) \quad (j=1,2,...,n \text{ and } i=1,2,...,m) \quad (24)$$

where a_{ji}: is the centre of A_{ji} and b_{ji}: is the width of A_{ji}.

In this research, four kinds of vector inputs (each one having lots of data for the time domain of training earthquake records), are used in order to design and train of AN-IT2FLC. The training earthquakes, which are used in this study, are eight arbitrary records of El Centro, Hachinohe, Kobe, Northridge, Loma prieta, Tabas, Morgan Hill and Erizkan records with different seismic properties. The characteristics of these ground accelerations shown in Figure 4 and Table 2.

Table 2. Specifications of earthquakes for training process of AN-IT2FLC

Earthquake	PGA	Duration (Sec)
El Centro	0.342g	50
Kobe	0.328g	69.98
Hachinohe	0.225g	35
Northridge	0.248g	59.98
Loma Prieta	0.112g	39.94
Tabas	0.852g	32.82
Morgan Hill	0.312g	39.97
Erzikan	0.515g	21.31

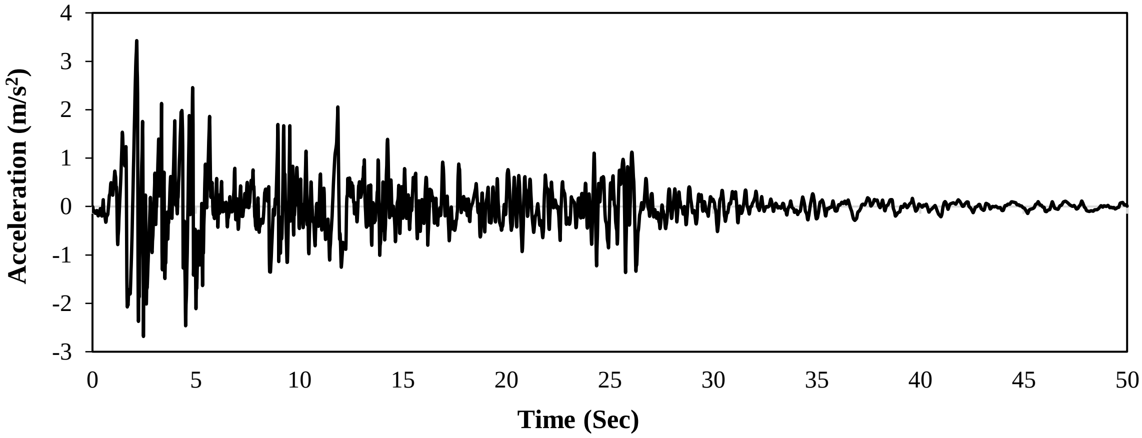

(a) El Centro

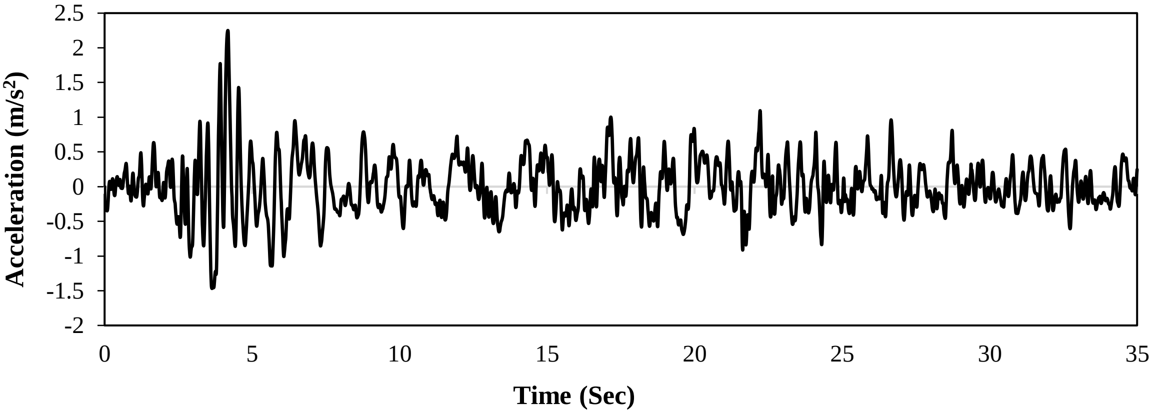

(b) Hachinohe

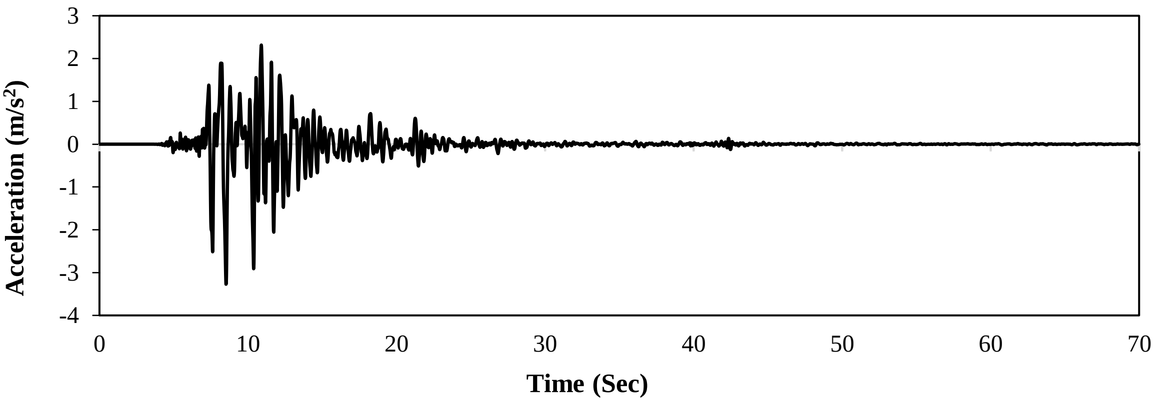

(C) Kobe

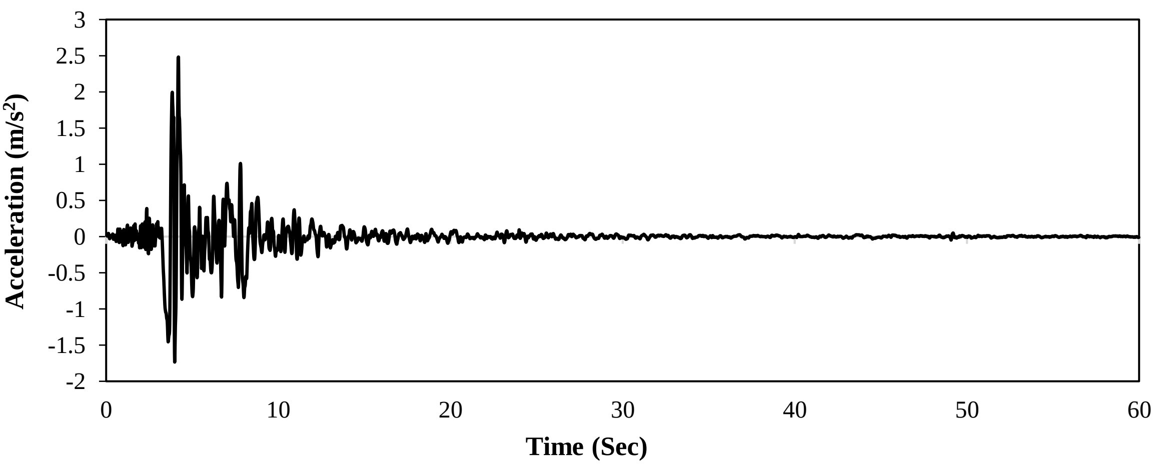

(d) Northridge

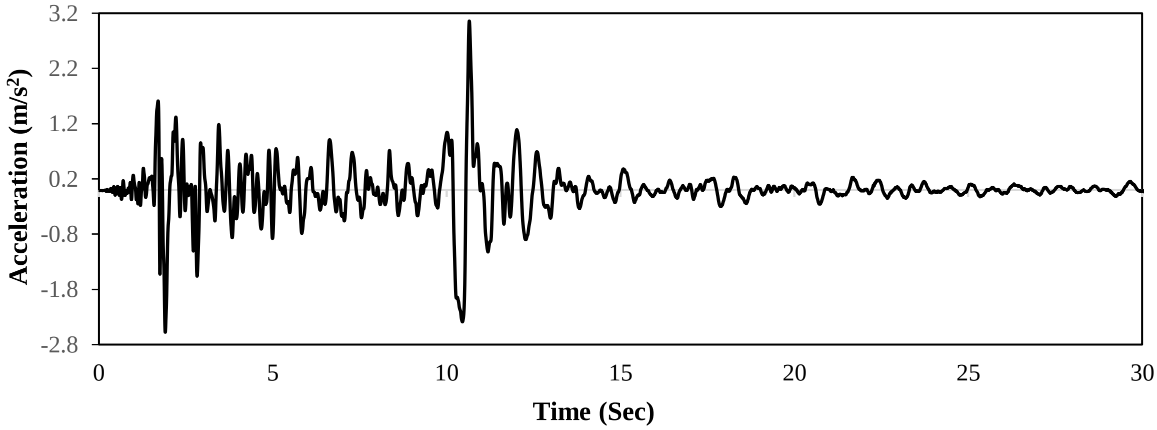

(e) Morgan Hill

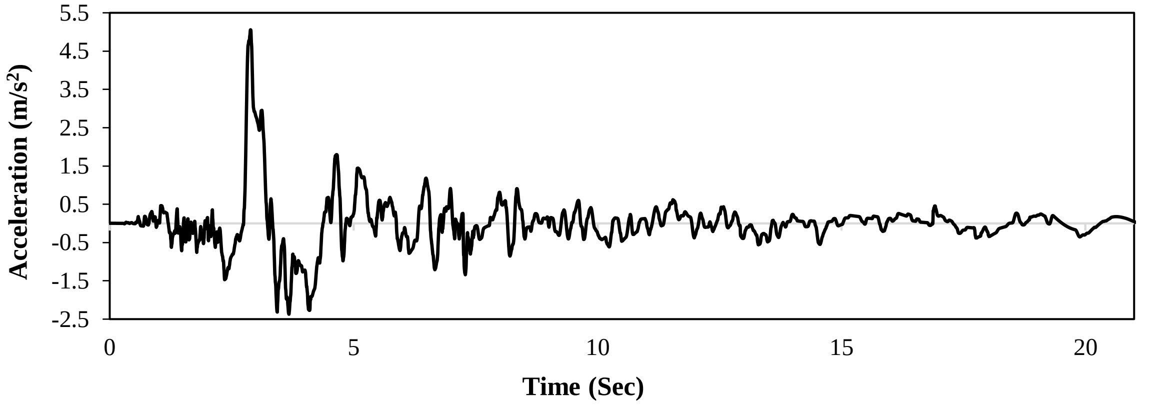

(f) Erizkan

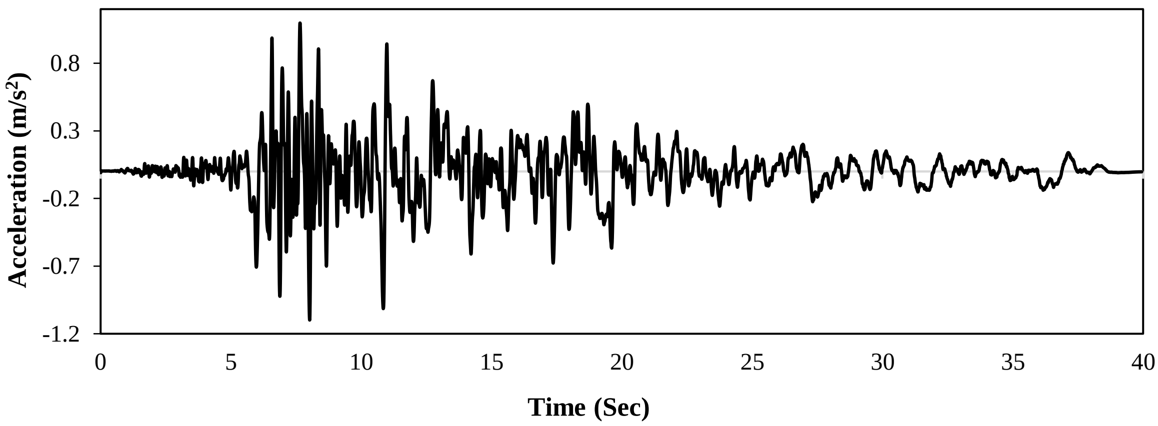

(g) LomaPrieta

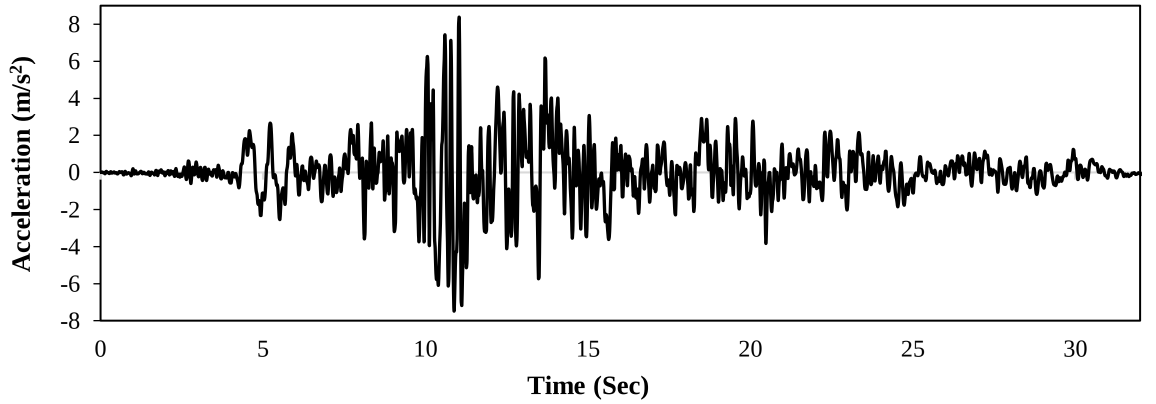

(h) Tabas

Fig. 4. Time history records of the eight earthquakes for training of AN-IT2FLC

The first two types of inputs are displacement and velocity of the building's top floor, which is controlled with an ATMD through IT2FLC under the seismic excitation. The third input, is the acceleration vector of mentioned earthquakes for the all instances of time domain records. The last input required for training of the proposed controller, is the IT2FLC control force vector of ATMD in the above-mentioned earthquakes. It is noteworthy that the associated data for designing of IT2FLC, such as the type and number of MFs of input and output variables and the fuzzy rule base, have been extracted from the research done by Golnargesi et al. (2014).

When an observation $x_1, x_2, \dots, x_n$: is given, according to simplified fuzzy reasoning method (Ichihashi, 1991), a fuzzy inference conclusion y can be obtained as follow:

First, for i=1, 2, …, m the agreement of i'th antecedent part is calculated using product operator:

$$h_i = A_{1i}(x_1)A_{2i}(x_2)\dots A_{ni}(x_n) = \prod_{j=1}^{n} A_{ji}(x_j)\,(i=1,2,\dots,m) \quad (25)$$

Then, a consequence y is calculated using center of gravity method as follows:

$$y = \left(\sum_{i=1}^{m} h_i y_i\right) / \left(\sum_{i=1}^{m} h_i\right) \quad (26)$$

The only output of mentioned algorithm of this research is the trained AN-IT2FLC control force.

When a training input-output datum $x_1, x_2, \dots, x_n$; y^*: is given for the fuzzy system model, it is well known to use the following objective function E for evaluating an error between y^* and y, which can be regarded as an optimum problem:

$$E = (y^* - y)^2/2 \quad (27)$$

where y^*: is a desired output value, and y: is a fuzzy inference result. In order to minimize the objective function E, a learning algorithm for updating the parameters (a_{ji}, b_{ji}, and y_i) has been proposed based on gradient descent algorithm as follows (Ichihashi, 1991; Kosko, 1992):

$$a_{ji}(t+1) = a_{ji}(t) - \frac{\alpha \partial E}{\partial a_{ji}(t)} = a_{ji}(t) - \alpha\left(\frac{\partial E}{\partial y}\right)\left(\frac{\partial y}{\partial h_i}\right)\left(\frac{\partial h_i}{\partial A_{ji}}\right)\left(\frac{\partial A_{ji}}{\partial a_{ji}(t)}\right) = a_{ji}(t) + \frac{2\alpha(y^* - y)(y_i - y)h_i(x_j - a_{ji})}{b_{ji}\sum_{i=1}^{m} h_i} \quad (28)$$

$$b_{ji}(t+1) = b_{ji}(t) - \frac{\beta \partial E}{\partial b_{ji}(t)} = b_{ji}(t) - \beta\left(\frac{\partial E}{\partial y}\right)\left(\frac{\partial y}{\partial h_i}\right)\left(\frac{\partial h_i}{\partial A_{ji}}\right)\left(\frac{\partial A_{ji}}{\partial b_{ji}(t)}\right) = b_{ji}(t) + \frac{\beta(y^* - y)(y_i - y)h_i(x_j - a_{ji})^2}{{b_{ji}}^2\sum_{i=1}^{m} h_i} \quad (29)$$

$$y_i(t+1) = y_i(t) - \frac{\gamma \partial E}{\partial y_i(t)} = y_i(t) - \gamma\left(\frac{\partial E}{\partial y}\right)\left(\frac{\partial y}{\partial_{y_i}(t)}\right) = y_i(t) + \frac{\gamma(y^* - y)h_i}{\sum_{i=1}^{m} h_i} \quad (30)$$

where a, β and γ: are the learning rates that are the constants in the learning process, and t: means the learning iteration. Consequently, the process of training and application of AN-IT2FLC is as follows in Figure 5.

According to this figure, when the controller training performed by above-mentioned algorithm in Matlab program (Figure 5a), it can be used for response reduction of structure in any earthquake record as in Figure 5b. The reference values shown in Figure 5b are the top story displacement and velocity of the building with zero quantities.

5. Result and Discussion

In the first part of results interpretation, accuracy of AN-IT2FLC design will be evaluated. This verification done through comparing the maximum controlled response of stories in the case of using proposed controller with similar values of uncontrolled, controlled responses with TMD, and controlled responses with ATMD through IT2FLC under the eight mentioned earthquake records. These result, are shown in Figure 6.

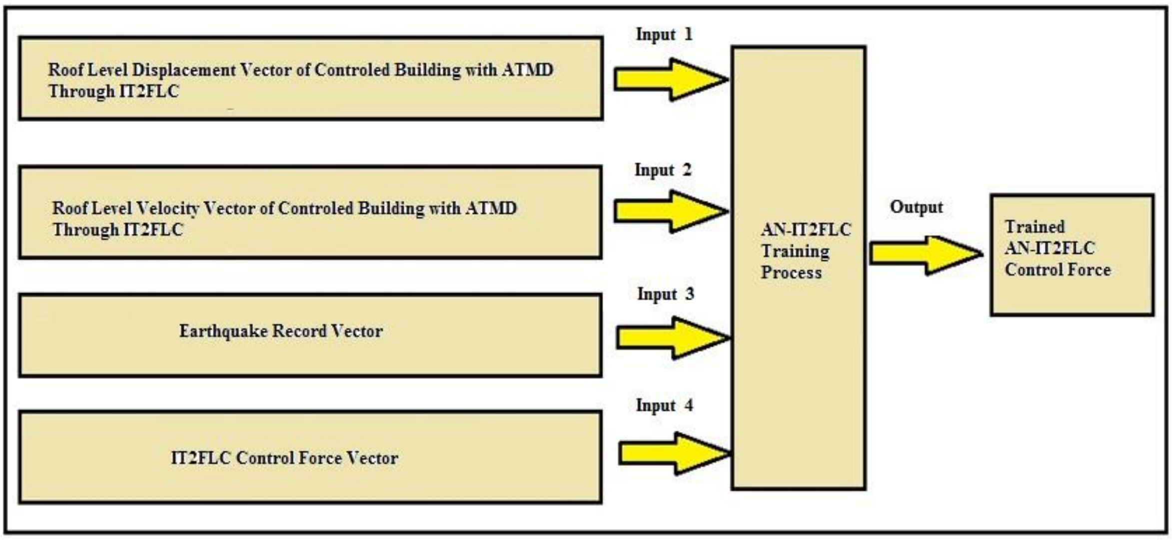

(a) Training

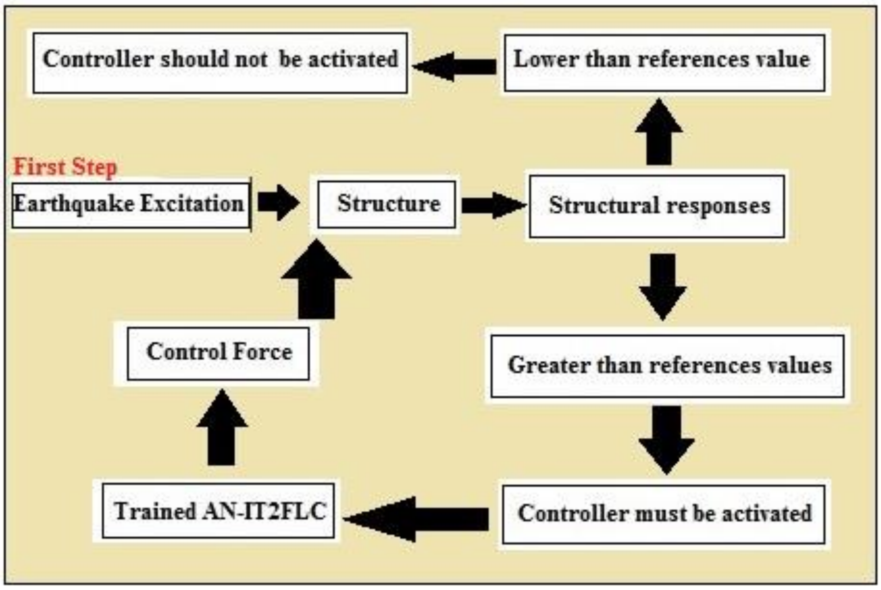

(b) Application

Fig. 5. Flowchart of AN-IT2FLC

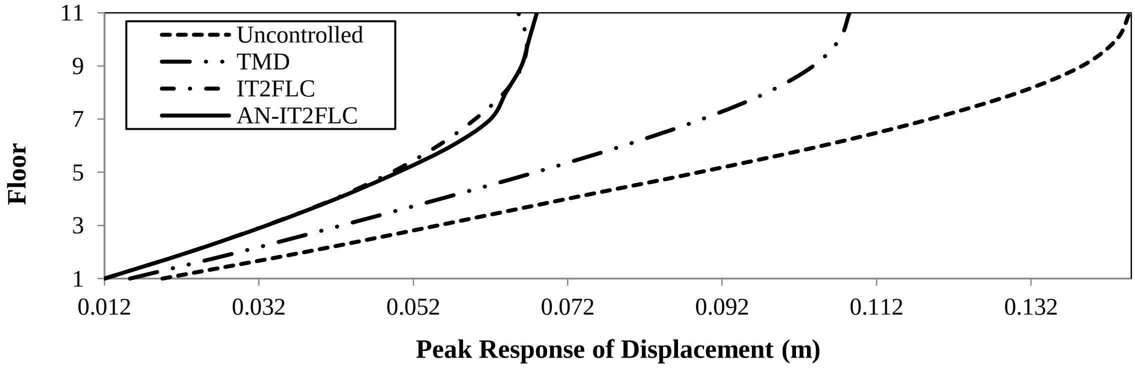

(a) El Centro

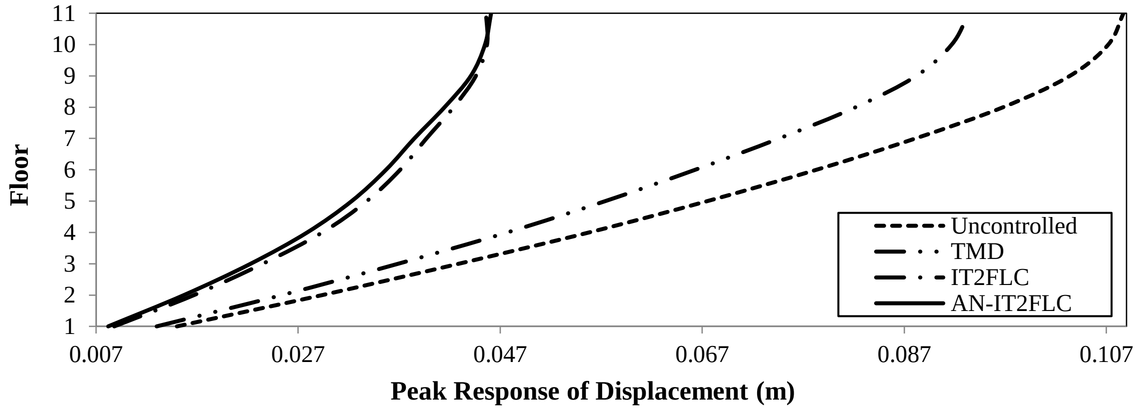

(b) Hachinohe

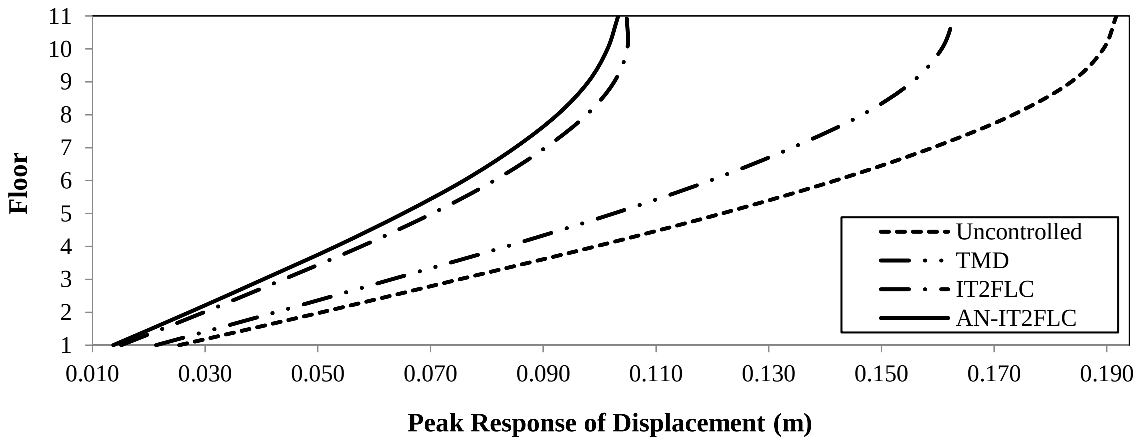

(C) Kobe

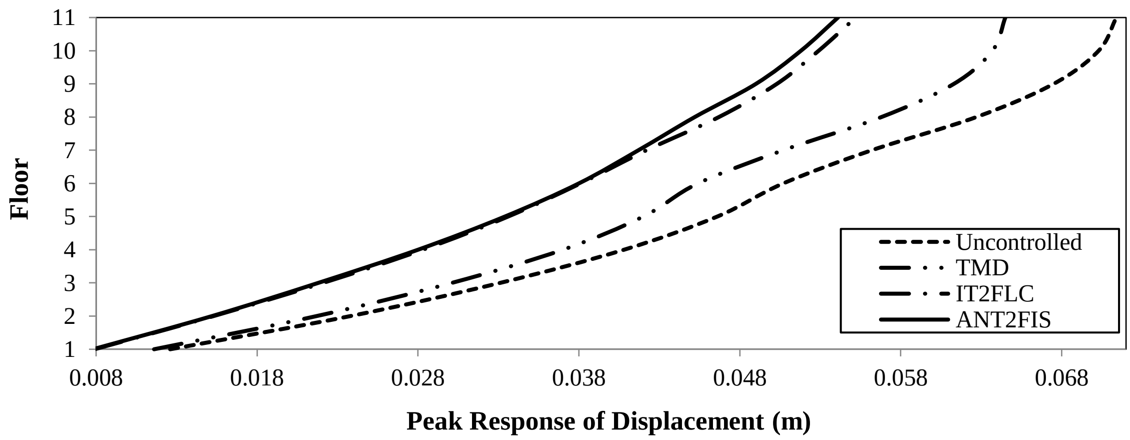

(d) Northridge

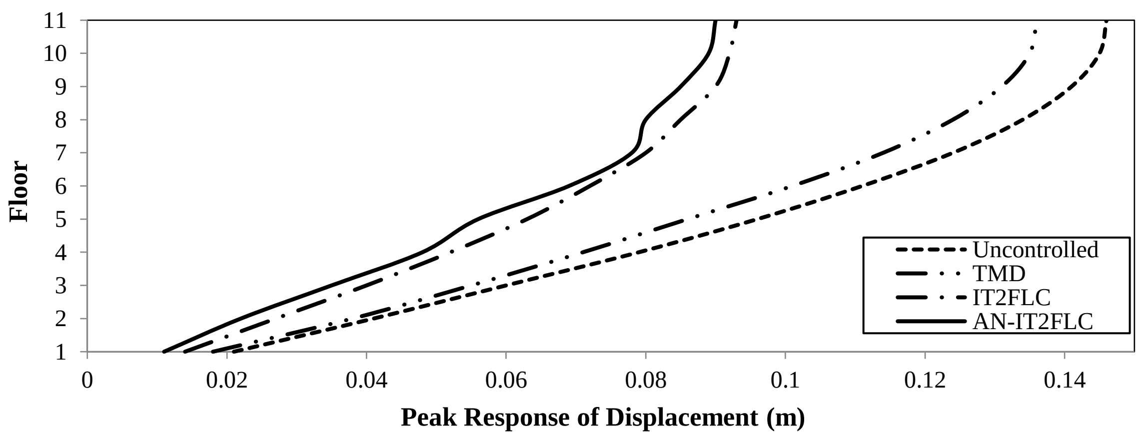

(e) MorganHill

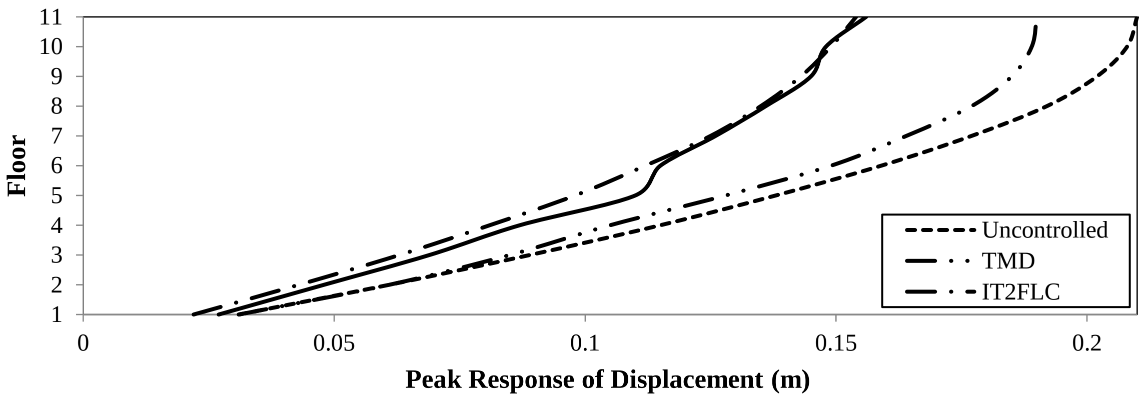

(f) Erizkan

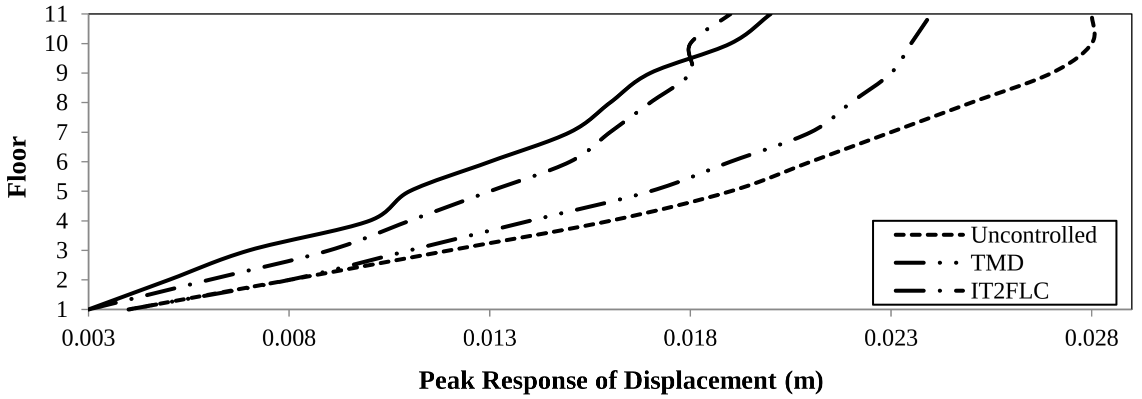

(g) Loma Prieta

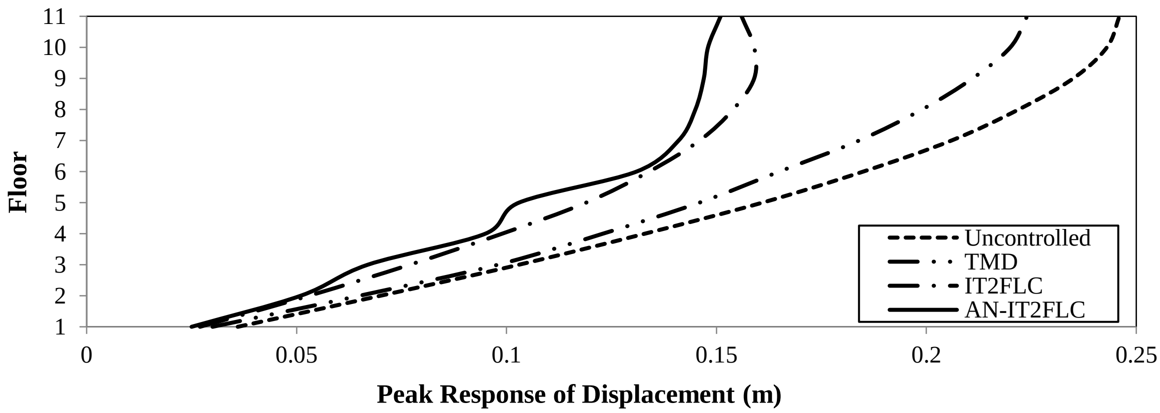

(h) Tabas

Fig. 6. Maximum displacement response of stories in different control cases for eight various ground accelerations

The results of peak response of displacement controlled with TMD are also presented for comparison. So the optimum parameters of TMD (damping ratio and tuning frequency ratio) are derived using Shuffled Complex Evolution (SCE) algorithm (Meshkat Razavi and Shariatmadar, 2015) in this study.

In the following, the steps for obtaining the optimum TMD parameters for the 11-storey shear building are described:

TMD is firstly designed to control the first modal displacement response of the mentioned building. Given the properties of the first mode that need to be controlled (Table 3) (Golnargesi et al., 2014), the TMD is designed in the same procedure as designing a TMD for a SDOF structure.

The mass ratio is defined as the damper mass to the first-mode modal mass as:

$$\mu = \frac{62.19 \times 10^3}{1057 \times 10^3} = 0.06$$

Table 3. Properties of the first mode of the 11-Story building (Golnargesi et al., 2014)

	Mass (Kg)	Damping ratio (%)
SDOF system	1057×10^3	5
Mass damper	62.19×10^3	7

Having known mass ratio (μ) and damping ratio (ξ) values, the optimum TMD parameters are obtained as (Meshkat Razavi and Shariatmadar, 2015):

$$\xi_{d_{opt}} = 0.1738 \text{ and } f_{OPT} = 0.9005$$

Now, the first-mode displacement response of 11-strory building can be controlled by the TMD. This completes the design procedure.

According to Figure 6 results show that the response reduction of AN-IT2FLC is more or the same as the IT2FLC in the eight earthquakes. Therefore, it can be concluded that the design of AN-IT2FLC is convenient.

The IT2FLC which is used in the previous part is designed based on two input variables each one having three upper and three lower Membership Functions (MFs) and one output variable. The main purpose of using two input variables for the IT2FLC is to show the efficiency of the fuzzy approach in the control problem. These input variables help in generating the inference rule base.

In this study, the inference rules have been developed by expert's knowledge and are shown in Table 4 and also the used specifications of IT2FLC have been given in Table 5.

The upper and lower MFs are triangular shaped and have been defined on the common interval [-1,1]. These MFs are shown in the Figure 7 of the manuscript as follows (Golnargesi et al., 2014):

Table 4. Inference rules for the IT2FLC (Golnargesi et al., 2014)

	Velocity		
Displacement	**N**	**Z**	**P**
N	PB	PM	PS
Z	PS	Z	NS
P	NS	NM	NB

Table 5. Specifications of IT2FLC (Golnargesi et al., 2014)

Aggregation	Maximum
Fuzzy Inference	Mamdani type
Type reducer	COS
Defuzzification	Center average

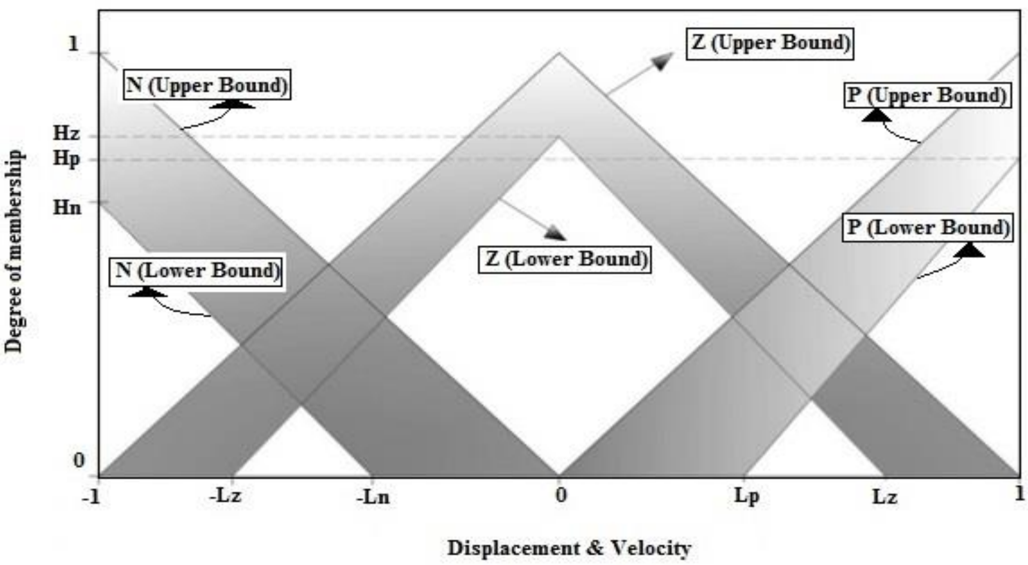

Fig. 7. Membership function of input parameters of IT2FLC (Golnargesi et al., 2014)

According to this figure, H_i and L_i ($i=z, n, p$) are the lower MF parameters. The peak responses of stories controlled with IT2FLC obtained based on adjusting of IT2FLC input parameters. In the other hand, to achieve the maximum response reduction of IT2FLC, the mentioned process must be done in any earthquake records. (Golnargesi et al., 2014).

This is one of the main deficiencies of IT2FLC, which it needs to adjust in any new ground acceleration. To increase the performance of IT2FLC in any new earthquake records, a numerical averaging method is used and general optimum parameters of IT2FLC, obtained based on the eight mentioned ground accelerations of the first part (Table 7).

Although the response reduction of IT2FLC with general parameters (General IT2FLC) is, less than that of the IT2FLC results of the first part, but is more practical in response reduction of structure for the new earthquakes.

So in the second part, in order to evaluate the efficiency of AN-IT2FLC, four other ground accelerations (Figure 8), including two far-field earthquakes (Kern-county and Chi-Chi) and two near-field earthquakes (Coalinga and Coyote-lake) are used and results are compared for different control states including uncontrolled and controlled by IT2FLC with general optimum parameters (Figure 9).

From the results, it can be concluded that ATMD with AN-IT2FLC reduces the peak displacement of building stories more than that of the ATMD through general IT2FLC for the Chi-Chi, Kern-county, Coyote-lake and Coalinga earthquakes. The corresponding response reduction at the roof level is about 18%, 16%, 9% and 7% for the mentioned earthquake records, respectively. In other words, comparing the response reduction of peak displacement of two types of controllers (AN-IT2FLC and general IT2FLC) revealed that the performance of the proposed controller is better than that of the IT2FLC.

Table 6. Adjusted parameters of IT2FLC for eight training earthquakes

Earthquake	**IT2FLC input parameters**					
	H_z	H_p	H_n	L_z	L_p	L_n
			Displacement			
El Centro	0.3	1	1	1	1	1
Hachinohe	0.3	1	1	0.3	1	1
Kobe	0.3	0.8	1	0.3	1	1
Northridge	1	1	0.3	1	1	1
Loma Perieta	1	0.3	1	1	1	1
Tabas	1	0.3	0.3	1	1	1
Erizkan	0.3	1	1	0.3	1	1
Morgan Hill	1	1	1	0.3	1	1
			Velocity			
El Centro	1	0.4	1	1	0.4	1
Hachinohe	1	0.4	0.4	1	0.4	0.4
Kobe	1	1	1	1	1	1
Northridge	1	0.3	0.3	1	1	1
Loma Perieta	1	1	1	1	1	1
Tabas	1	0.3	1	1	1	1
Erizkan	0.3	1	1	0.3	1	1
Morgan Hill	1	1	1	0.3	1	1

Table 7. General optimum parameters of IT2FLC

General parameters of IT2FLC					
Hz	***Hp***	***Hn***	***Lz***	***Lp***	***Ln***
		Displacement			
0.65	0.8	0.85	0.65	1	1
		Velocity			
0.9	0.65	0.85	0.85	0.85	0.95

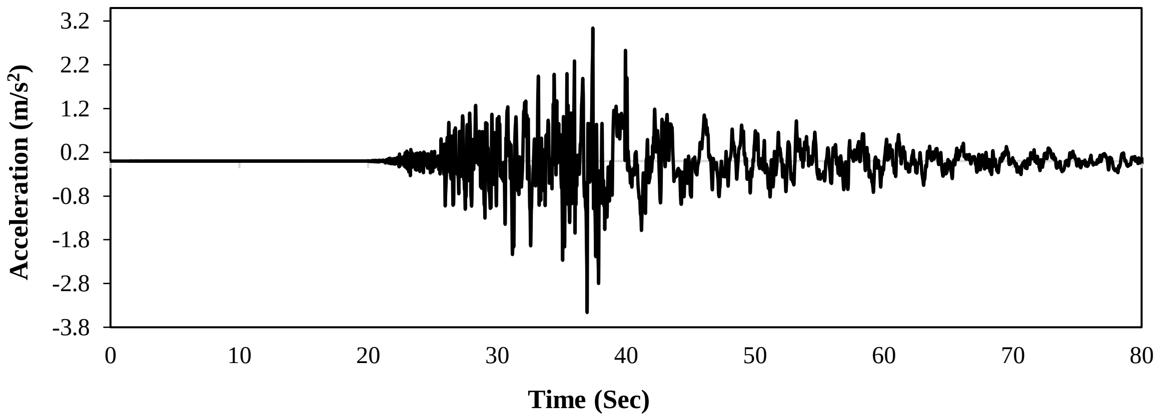

(a) Chi-Chi

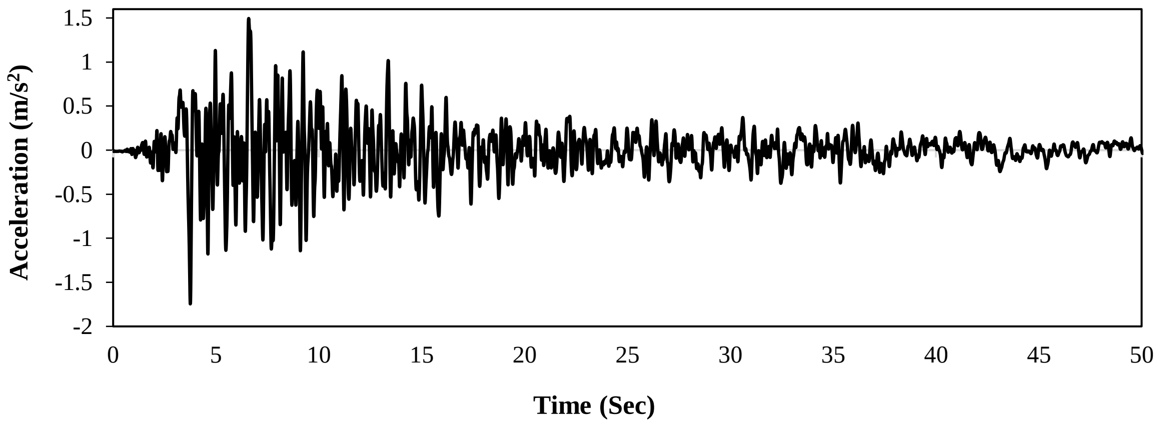

(b) Kern-county

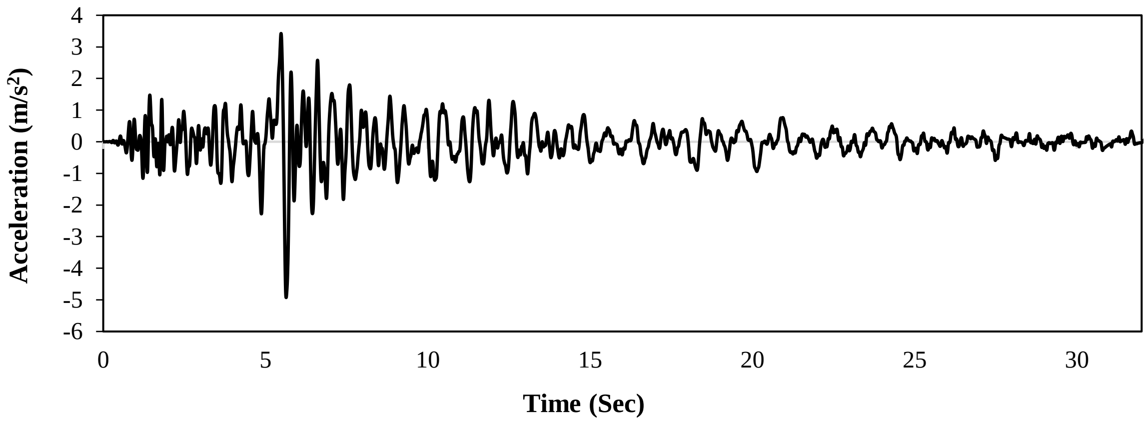

(C) Coyote-lake

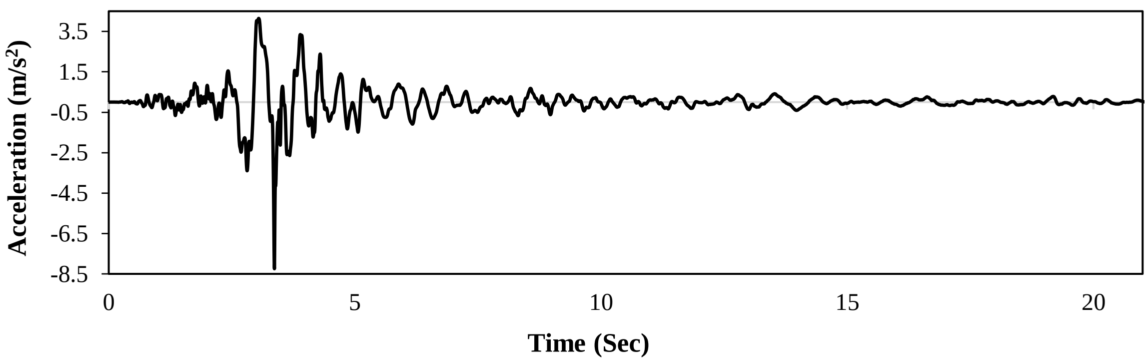

(d) Coalinga

Fig. 8. Near-field and far-field ground acceleration records used in this study to investigate the efficiency of AN-IT2FLC

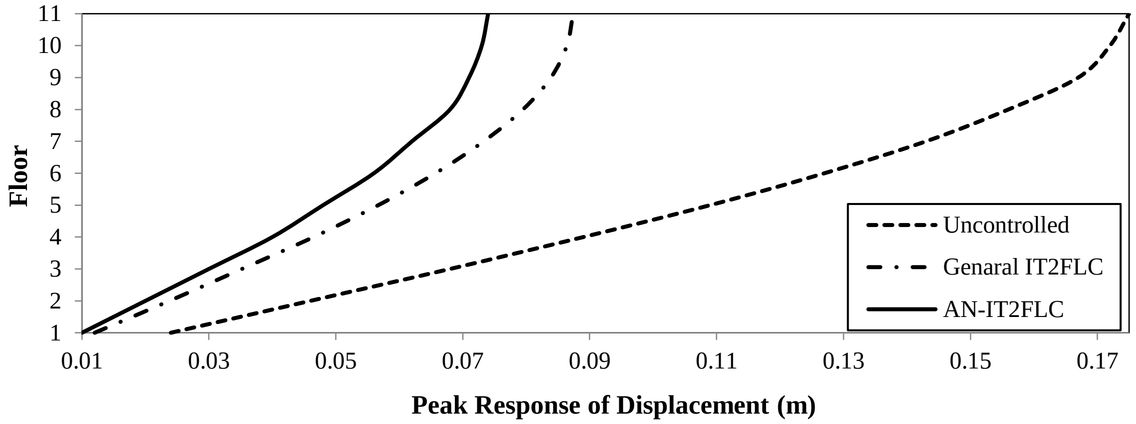

(a) Chi-Chi

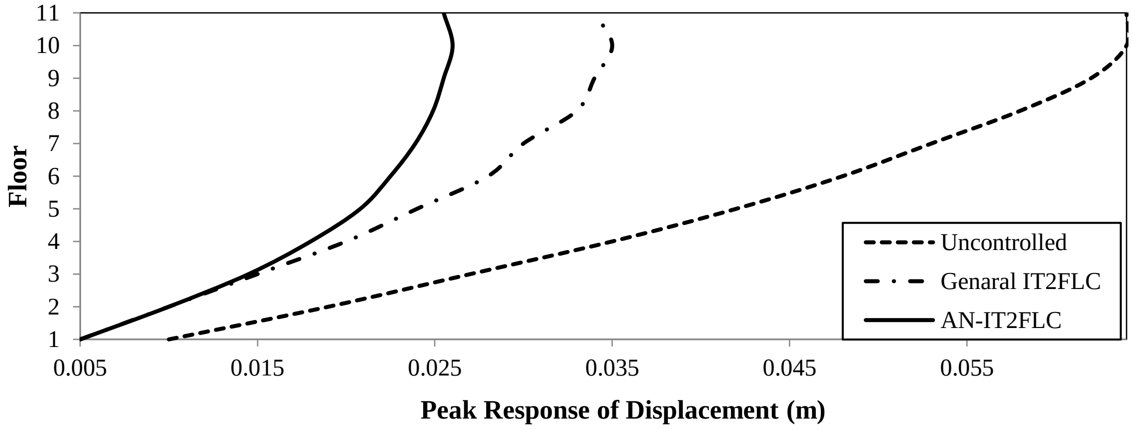

(b) Kern-county

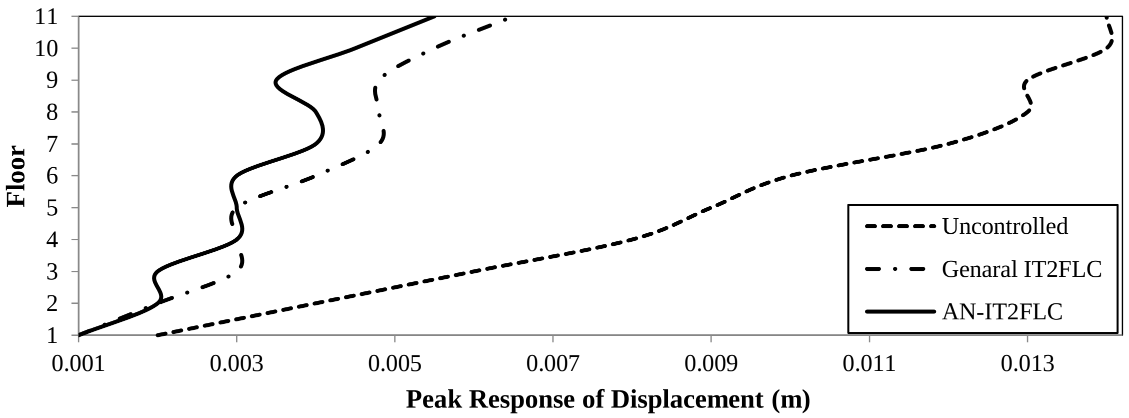

(C) Coyote-lake

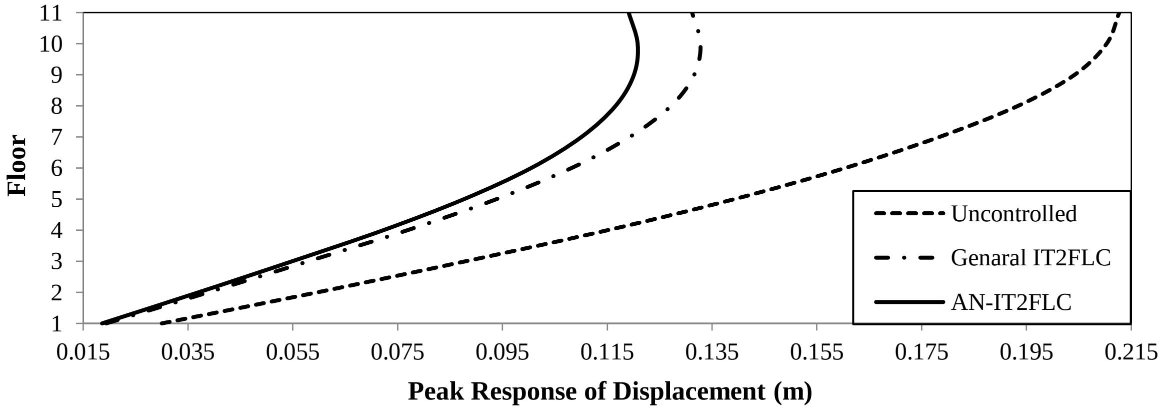

(d) Coalinga

Fig. 9. Peak displacement response of stories for various control systems and different earthquakes

In fact, one of the main reasons for the superiority of the proposed controller is its compatibility in different seismic conditions. In the other words, the AN-IT2FLC, only once trained for a number of optional earthquakes and then the proposed controller with adjusted parameters can be used to mitigate the structural response in any desired ground accelerations with a much higher speed and more response reduction than those obtained by IT2FLC.

The displacement time response of top floor is also calculated and compared in two modes of controlled with ATMD through general IT2FLC and AN-IT2FLC and different ground accelerations (Figure 10).

By comparing the results of time responses of building' top floor in the case of using two types of controllers, it is concluded that the controlled responses obtained with ATMD through AN-IT2FLC is less than that of the General IT2FLC. The response reduction is more for far field ground accelerations (Chi-Chi and Kern-county records).

Another and more precise criteria for assessing and comparing the performance of both ATMD controllers (AN-IT2FLC and general IT2FLC) in term of time response reduction, is the controlled Integral Square Error (ISE) displacement of top floor (Figure 11).

Comparing the values of controlled displacement ISE of two controllers, revealed that the obtained response reduction of the proposed controller is more than that of the IT2FLC in mentioned earthquake records.

Although a visual comparison of responses in Figures 10 and11 indicates the superiority of the proposed controller in the time history and ISE displacement responses of top floor, however for a quantitative review, a comparison between the mentioned responses has been done in Tables 8 and 9 in the term of maximum responses of time history and the average ISE response reduction, respectively.

Table 8. Peak response of top floor displacement (m)

General IT2FLC	AN-IT2FLC	General IT2FLC	AN-IT2FLC
Chi-Chi		Kern-county	
0.087	0.071	0.034	0.028
Coyote-lake		Coalinga	
0.0028	0.0025	0.106	0.098

Table 9. Average ISE response reduction of AN-IT2FLC to general IT2FLC at the top floor (%)

Chi-Chi	Coyote-lake	Coalinga	Kern-county
22	11	10	13

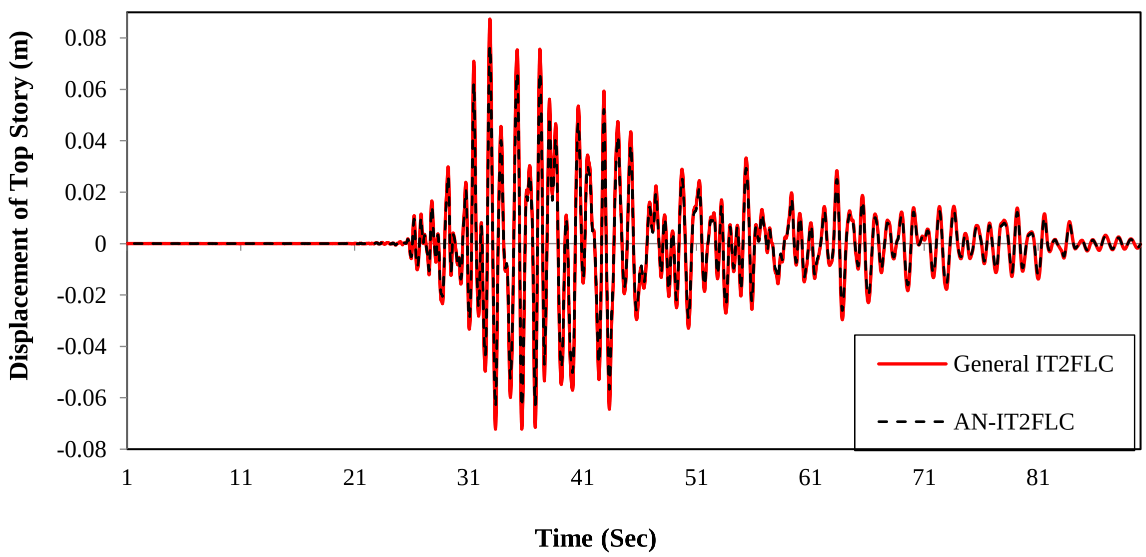

(a) Chi-Chi

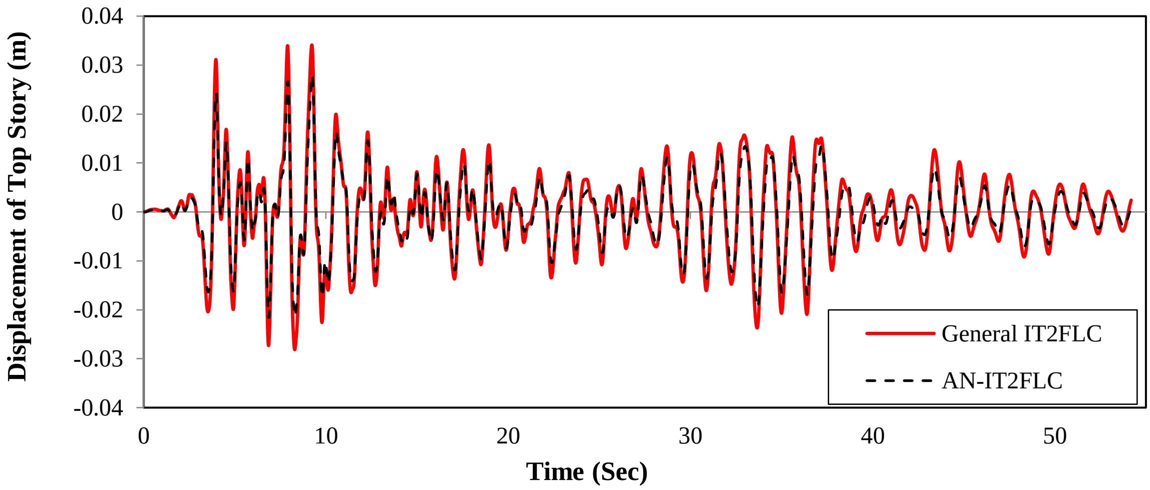

(b) Kern-county

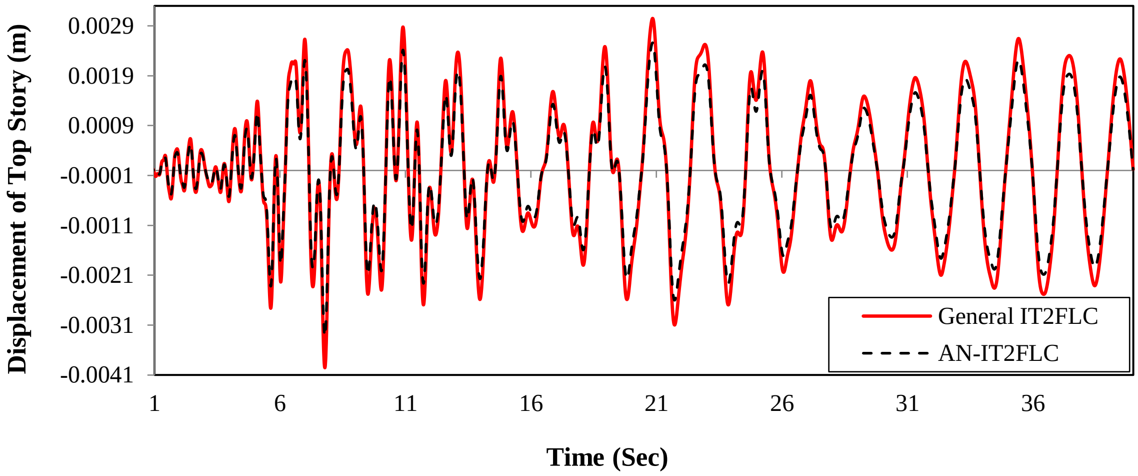

(C) Coyote-lake

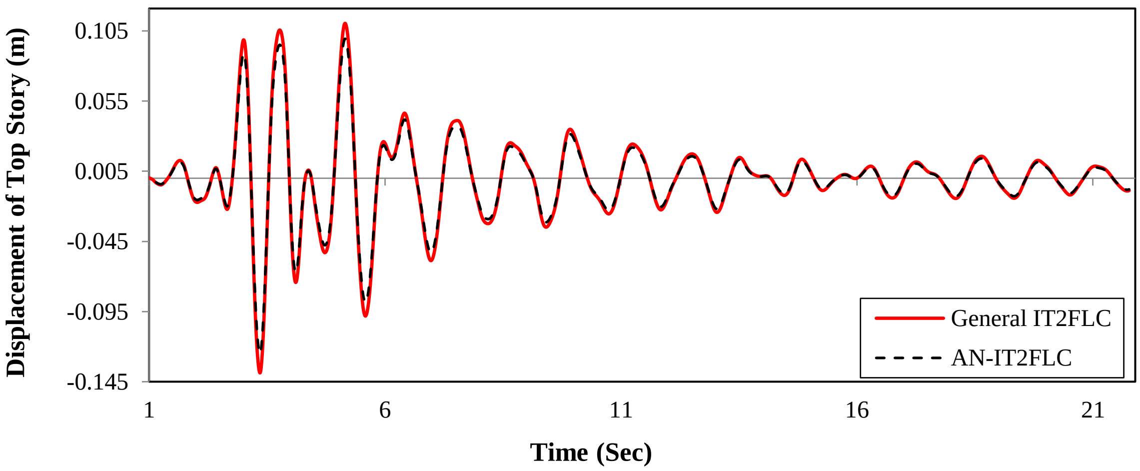

(d) Coalinga

Fig. 10. Comparison of controlled time history response of roof level with ATMD through IT2FLC and AN-IT2FLC for different earthquake

It is seen from the first table that AN-IT2FLC reduces the peak response of top floor more than that of the general IT2FLC and are about 18%, 16%, 9% and 7% for the Chi-Chi, Kern-county, Coyote-lake and Coalinga earthquakes. From the results, it can be seen that the most and the least response reductions belong to the Chi-Chi and Coalinga ground accelerations, respectively.

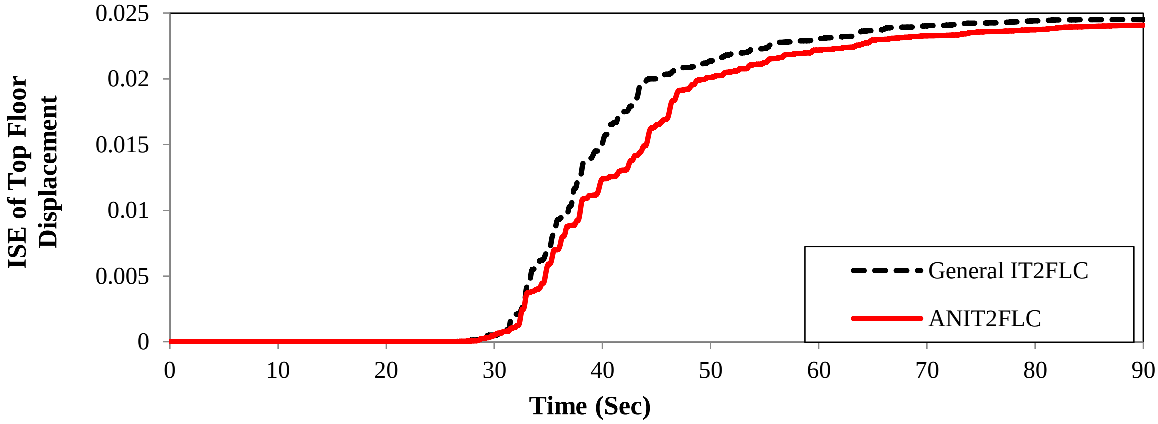

(a) Chi-Chi

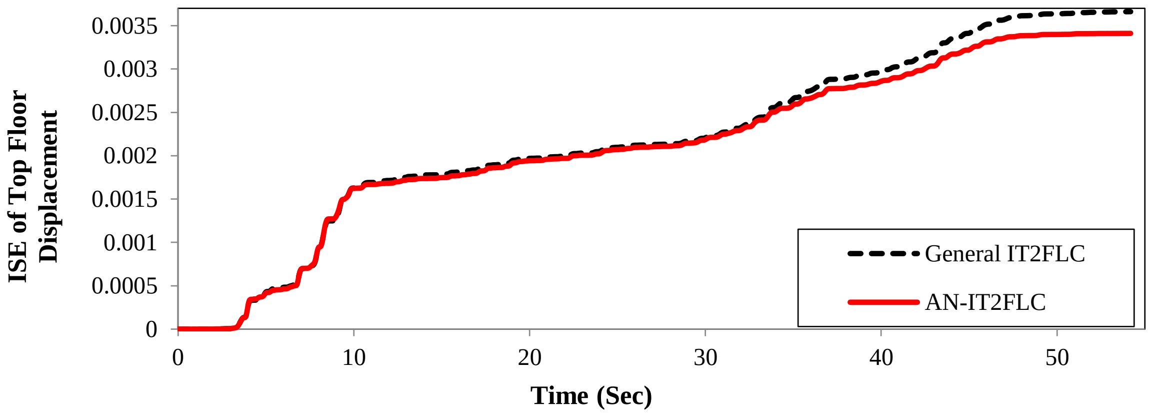

(b) Kern-county

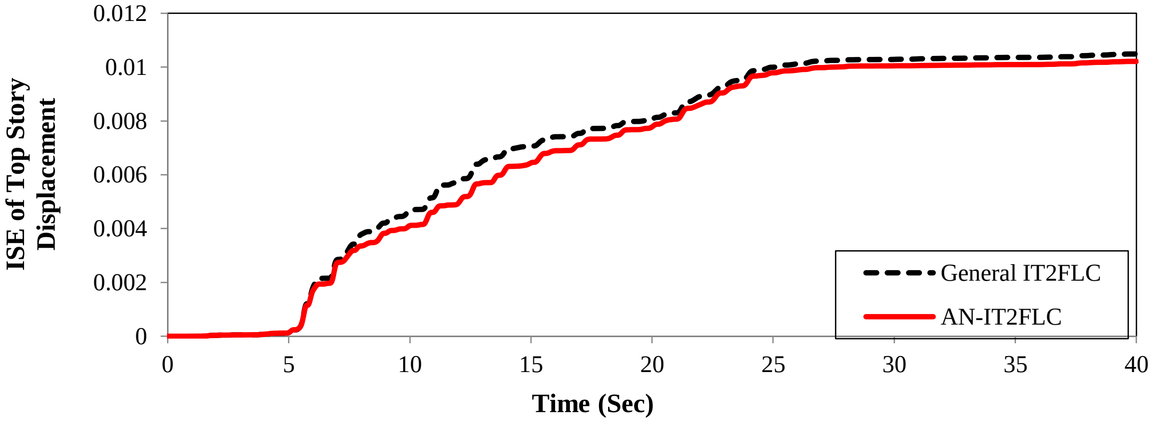

(C) Coyote-lake

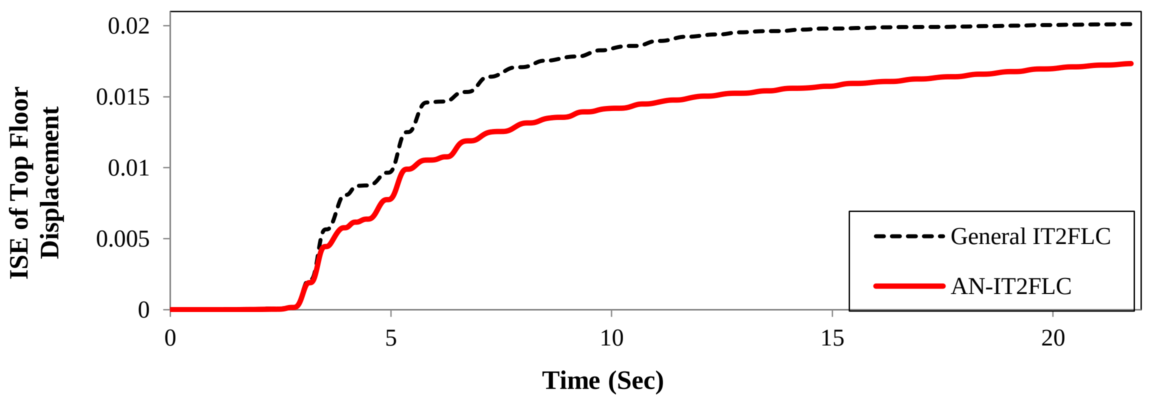

(d) Coalinga

Fig. 11. Comparison of controlled ISE of roof level with ATMD using AN-IT2FLC and IT2FLC for different earthquake

Another criterion for comparison of controlled time history responses is the ISE displacement of the top floor. For a quantitative interpretation of the results which are presented in Figure 11, the percentage of the average ISE response reduction of AN-IT2FLC to general IT2FLC are also calculated and is provided in the last table.

According to Table 9 it can be seen that the most and the least percentage of average response reduction of ISE are 22% and 10% for the Chi-Chi and Coalinga ground earthquakes, respectively. In the last part of results, the corresponding values of maximum control forces are shown in Table 10.

Table 10. Comparison of maximum control force of AN-IT2FLC and General IT2FLC for different earthquakes

Earthquake	**Maximum control force (kN)**	
	General IT2FLC	**AN-IT2FLC**
Chi-Chi	390	483
Kern-county	610	641
Coalinga	1120	1250
Coyote-lake	490	520

According to Table 10, it can be realized that the peak value of active control force in AN-IT2FLC is little more than the general IT2FLC in most earthquake records. Furthermore, from the results it can be understood that the highest values of control force in both controllers belongs to Coalinga earthquake record compared to other ground accelerations. This is due to the pulse-like feature of Coalinga record, which the most active actuator mechanism occurs under the influence of this earthquake.

6. Conclusions

This research is one of the first studies conducted on the use of AN-IT2FLC in an ATMD. One of the main disadvantages of the IT2FLC is its dependence on adjust and optimize parameters in each earthquake record, in order to achieve the maximum response reduction. However, this defect has been addressed in the proposed controller using the neural network training process. In this study, an 11-story shear building with an ATMD on its roof level was used to evaluate the performance of AN-IT2FLC. The proposed controller was initially trained using eight earthquakes with various seismic specifications. Then, the controller efficiency was evaluated using two far-field earthquakes (Chi-Chi and Kern-county) and two near-field earthquakes (Coalinga and Coyote-lake). Various results of this analysis were obtained, which are summarized as following:

- AN-IT2FLC does not need to adjust and optimize the fuzzy MFs parameters, in each earthquake records. In other words, the controller parameters trained only once for a given number of arbitrary earthquakes and the most structural response reduction obtained with much higher speed and accuracy rather than other earthquakes.
- By comparing the maximum response of the stories, it concluded that the proposed controller has a greater response reduction, rather than General IT2FLC. The most response reduction of AN-IT2FLC rather than General IT2FLC occurred in the Chichi earthquake and was about 18%.
- Evaluating the ISE responses indicates that ATMD with AN-IT2FLC reduces the time response of top floor more than that of ATMD through general IT2FLC in most earthquakes.
- Comparison of maximum control force in two types of controllers (AN-IT2FLC and general IT2FLC) indicates that the proposed controller has a little more values, compared to the general IT2FLC.

7. References

Anajafi, H. and Medina, R. (2017). “Comparison of the seismic performance of a partial mass isolation technique with conventional TMD and base-isolation systems under broad-band and narrow-band excitation”, *Engineering*

Structures, 158(3),110-123.

Bargi, K., Kave, A., Lucas, C. and Rahami, H. (2012). "Generation of artificial earthquake accelerograms using wavelet and neural networks", *Sharif Journal of Civil Engineering*, 2-28(3), 79-88.

Bakhshinezhad, S. and Mohebbi, M., (2019). "Multiple failure criteria-based fragility curves for structures equipped with Satmds", *Earthquake and Structure*, 17(5), 463-475.

Bathaei, A. Ramezani, M. and Ghorbani, A., (2017). "Type-1 and Type-2 fuzzy logic control algorithms for semi-active seismic vibration control of the College Urban Bridge using MR dampers", *Civil Engineering Infrastructures Journal*, 50(2), 331-351.

Boccamazzo, A., Carboni, B. and Quaranta, G. (2020). "Seismic effectiveness of hysteretic tuned mass dampers for inelastic structures", *Engineering Structures*, 216, 110591.

Chang, J.C.H. and Soong, T.T. (1980). "Structural control using active tuned mass dampers", *Engineering Mechanics Division*, 106(6), 1091-1098.

Collins, R. and Basu, B. (2006). "Control strategy using bang-bang and minimax principle for FRF with ATMDs", *Engineering Structures*, 28(3), 349-356.

Chen, T., Bird, A., Muḥammad, J.M., Cao, S.B., Melvilled, C. and Cheng, C.Y.J., (2019). "Prediction and control of buildings with sensor actuators of fuzzy EB algorithm", *Earthquakes and Structures*, 17(3), 307-315.

Chopra, A.K., (2001). *Dynamics of structures-theory and applications to earthquake engineering*, 2nd Edition, Prentice-Hall, 472-496.

Farshidianfar, A. and Soheili, S. (2013). "Ant colony optimization of tuned mass dampers for earthquake oscillations of high rise structures including soil–structure interaction", *Soil Dynamic and Earthquake Engineering*, 51, 14-22.

Guclu, R. and Yazici, H. (2008). "Vibration control of a structure with ATMD against earthquake using fuzzy logic controllers", *Sound and Vibration*, 318(1-2), 36-49.

Golnargesi, S., Shariatmadar, H., Meshkat Razavi, H. (2018). "Seismic control of building with active tuned mass damper through interval type-2fuzzy logic controller including soil-structure interaction", *Asian Journal of Civil Engineering*, 19(2), 177-188.

Housner, G.W., Bergman, L.A., Caughey, T.K., Chassiakos, A.G., Claus, R.O., Masri, S.F., Skelton, R.E., Soong, T.T., Spencer Jr., B.F. and Yao, T.P. (1997). "Structural control: Past, present, and future", *Journal of Engineering and Mechanics*, ASCE, 123(9), 897-971.

Huang, H., Mosalam, K.M. and Chang, W.S. (2020). "Adaptive tuned mass damper with shape memory alloy for seismic application", *Engineering Structures*, 223, 111171.

Ichihashi, H. (1991). "Iterative fuzzy modeling and a hierarchical network", *Proceedings of the 4th IFSA Congress, Engineering,* Brussels, 49-52.

Jang, J.R. (1993), "Adaptive-network-based fuzzy inference system", *IEEE Transactions on Systems, Man, and Cybernetics*, 23(3), 665-685.

Jin, C., Chung, W.C., Kwon, D.S. and Kim, M.H. (2020). "Optimization of tuned mass damper for seismic control of submerged floating tunnel", *Engineering Structures*, 241, 112460.

Kobori, T., Koshika, N., Yamada, K. and Ikeda, Y. (1991). "Seismic response controlled structure with active mass driver system, Part 1: Design", *Earthquake Engineering and Structure Dynamics*, 20(2), 133-149.

Kosko, B. (1992). *Neural Networks and fuzzy systems*, Prentice Hall, Englewood Cliffs.

Liangkun, W., Weixing, S., Ying, Z. and Quanwu, Z., (2020). "Semi-active eddy current pendulum tuned mass damper with variable frequency and damping", *Smart Structures and Systems*, 25(1), 65-80.

Liangkun,W., Weixing, S. Ying, Z., (2019). "Study on self-adjustable variable pendulum tuned mass damper", *The Structural Design of Tall and Special Buildings*, 28(1), 1561.

Liangkun,W., Weixing, S. Xiaowei, L., Quanwu, Z., Ying, Z., (2019)."An adaptive-passive retuning device for a pendulum tuned mass damper considering mass uncertainty and optimum frequency", *Structural Control and Health Monitoring*, 26(7), e2377.

Liangkun,W., Nagarajaiah, S, Weixing, S, Ying, Z., (2020). "Study on adaptive-passive eddy current pendulum tuned mass damper for wind-induced vibration control", *The Structural Design of Tall and Special Buildings*, 29(15), e1793.

Love, J.S. and Haskett, C. (2019). "Measuring inherent structural damping of structure-TMD systems", *Engineering Structures*, 196(3), 109-300.

Lievens, K., Lombaert, G. and De Roeck, G. (2016). "Robust design of a TMD for the vibration serviceability of a footbridge", *Engineering Structures*, 123, 408-418.

Meshkat R.H. and Shariatmadar, H. (2015). "Optimum parameters for tuned mass damper using Shuffled Complex Evolution (SCE) algorithm", *Civil Engineering Infrastructures Journal*, 48(1), 83-100.

Miguel, L., Lopez, R. and Torii, A. (2016). "Robust design optimization of TMDs in vehicle–bridge coupled vibration problems", *Engineering Structures*, 126, 703-711.

Naderpour.H, Vosughifar,H. and Ghobakhloo, E. (2016). "Evaluation of effective parameters on wave diffraction of far-fault ground motions using artificial neural networks", *Sharif Journal*

of Civil Engineering, 32-2(1), 13-23.
Pourzeynali, S., Lavasani, H.H. and Modarayi, A.H. (2007). “Active control of high rise building structures using fuzzy logic and genetic algorithms”, *Engineering Structure*, 29(3), 346-357.
Soong,T.T, Spencer, B.F. (2002). “Supplemental energy dissipation: state-of-the-art and state-of-the-practice”, *Engineering Structure*, 24(3), 243-259.
Shariatmadar, H., Golnargesi, S. and Akbarzadeh Totonchi, M.R. (2014). “Vibration control of buildings using ATMD against earthquake excitations through Interval Type-2 Fuzzy Logic Controller”, *Asian Journal of Civil Engineering*, 15(3), 321-338.
Spencer Jr, B.F. and Nagarajaiah, S. (2003).” State of the art of structural control”, *Journal of Structural Engineering*, ASCE, 129, 845-856.
Wang, L., Nagarajaiah, S., Shi, W. and Zhou, W. (2021). “Semi-active control of walking-induced vibrations in bridges using adaptive tuned mass damper considering human-structure-interaction”, *Engineering Structures*, 244, 112743.
Yager, R.R. and Filev, D.P. (1994). “Generation of fuzzy rules by mountain clustering”, *International Journal of Intelligent and Fuzzy Systems*, 2(3), 209-219.
Yager, R.R. and Filev, D.P. (1994). *Essentials of fuzzy modeling and control*, John Wiley & Sons.
Zuo, H., Bi, K., Hao, H. and Ma, R. (2021). “Influences of ground motion parameters and structural damping on the optimum design of inerter-based tuned mass dampers”, *Engineering Structures*, 227, 111422.

This article is an open-access article distributed under the terms and conditions of the Creative Commons Attribution (CC-BY) license.